frontiers | Frontiers in Astronomy and Space Sciences

TYPE Original Research
PUBLISHED 02 December 2024
DOI 10.3389/fspas.2024.1412323



OPEN ACCESS

EDITED BY
Derek L. Buzasi,
Florida Gulf Coast University, United States

REVIEWED BY
Sergio B. Fajardo-Acosta,
California Institute of Technology,
United States
Scott Wolk,
Harvard University, United States

*CORRESPONDENCE
Fatemeh Bagheri,
fatemeh.bagheri@nasa.gov

RECEIVED 04 April 2024
ACCEPTED 07 November 2024
PUBLISHED 02 December 2024

CITATION
Bagheri F, Garga A and Lopez RE (2024) Exploring radio emissions from confirmed exoplanets using SKA.
*Front. Astron. Space Sci.* 11:1412323.
doi: 10.3389/fspas.2024.1412323



# Exploring radio emissions from confirmed exoplanets using SKA

Fatemeh Bagheri[1,2]*, Anshuman Garga[2] and Ramon E. Lopez[2]

[1]NASA Goddard Space Flight Center, Greenbelt, MD, United States, [2]Department of Physics, University of Texas at Arlington, Arlington, TX, United States

Our understanding of magnetic fields in exoplanets remains limited compared to those within our solar system. Planets with magnetic fields emit radio signals primarily due to the Electron Cyclotron Maser Instability mechanism. In this study, we explore the feasibility of detecting radio emissions from exoplanets using the Square Kilometre Array (SKA) radio telescope. Utilizing data from the NASA Exoplanet Archive, we compile information on confirmed exoplanets and estimate their radio emissions using the RBL model. Our analysis reveals that four exoplanets—Qatar-4 b, TOI-1278 b, CoRoT-10 b, and HAT-P-20 b—potentially exhibit radio signals suitable for observation with the SKA telescope.

KEYWORDS

**planetary radio emissions, ECMI, RBL model, SKA, confirmed exoplanets**

## 1 Introduction

Observing and measuring the magnetic fields of exoplanets holds paramount importance in contemporary astrophysical research. The magnetic field of a planet serves as a fundamental aspect of its physical makeup, providing crucial insights into its internal structure and dynamical processes. Understanding exoplanetary magnetic fields allows for the investigation of planetary interiors, shedding light on the presence of metallic cores and the mechanisms driving magnetic field generation, such as dynamo processes. Additionally, the interaction between a planet's magnetic field and the surrounding stellar wind profoundly influences its atmospheric dynamics, including the retention and loss of atmospheric gases. This interplay is pivotal in determining a planet's habitability and its potential to support life as we know it. Furthermore, studying exoplanetary magnetic fields offers a glimpse into the diverse array of planetary systems beyond our own, enriching our understanding of planetary formation and evolution across different stellar environments and orbital configurations.

However, the task of observing and measuring the magnetic field of exoplanets presents a significant challenge. The magnetospheres of several solar system bodies, such as Earth, Jupiter, Saturn, Uranus, and Neptune, manifest distinct patterns of non-thermal continuum radiation emission due to their interaction with the solar wind (Zarka, 1998). The electron cyclotron maser instability (ECMI) mechanism is believed to be the primary source of non-thermal radio emission in planetary magnetospheres, where energetic electrons emit coherent radiation along magnetic field lines (Melrose and Dulk, 1982; Dulk, 1985). Observations of such emissions provide valuable insights into the strength and configuration of exoplanetary magnetic fields. However, despite extensive efforts, direct detection of radio emissions from exoplanets has proven challenging due to the low sensitivity of ground-based radio telescopes (Murphy et al., 2015; Lazio et al., 2018; Turner et al., 2021). Recent advancements, particularly in the development of next-generation instruments like the Square Kilometre Array (SKA), offer promising opportunities for more sensitive and

comprehensive observations of exoplanetary radio emissions. The leading contemporary ground-based telescope for detecting planetary radio emissions will be the SKA telescope. Comprising two arrays, SKA1-Low and SKA1-Mid, it covers a broad frequency range from 50 MHz to 14 GHz. With its immense collecting area, totaling one square kilometer when fully operational, the SKA will be able to capture faint radio signals (Lazio et al., 2009). By detecting and characterizing exoplanetary radio emissions, we can gain deeper insights into the magnetic properties, atmospheric dynamics, and potentially the presence of exomoons in exoplanetary systems.

To date, the confirmed count of exoplanets has reached 5,765. In this study, we conduct an assessment of the non-thermal radio emissions originating from these exoplanets, utilizing the Radiometric Bode's Law (RBL model) (Zarka et al., 2001; Zarka, 2004; Zarka, 2007). Subsequently, we identify potential candidates for detection using the Square Kilometre Array (SKA) telescope. The structure of the paper is as follows: Section 2 outlines the methodology used to estimate the exoplanetary emissions. In Section 3, we present the results of our findings, and Section 4 contains our conclusions.

# 2 Methodology

## 2.1 Estimation of exoplanets radio emission

Observations of magnetized planets within our Solar System have revealed a consistent relationship between the power of auroral emissions and the energy flux of the incoming stellar wind (Zarka et al., 2001; Zarka, 2004; 2007; Zarka et al., 2018). This phenomenon extends to various planetary bodies, including those with Jovian satellite and their host radio emissions (Noyola et al., 2014; 2016). Specifically, studies have shown that approximately 1% of the energy carried by electrons in these systems manifests as radio waves (Zarka et al., 2018). This correlation between auroral emissions and stellar wind energy flux, along with the strength of the planetary magnetic field, is encapsulated by the RBL model (Zarka et al., 2001; Zarka, 2004; Zarka, 2007). Mathematically, this model relates the radio power from an exoplanet to the incident power of the stellar winds, as expressed by

$$P_{rad} = 4\times10^{18} erg\ s^{-1}\left(\frac{\dot{M}_{ion}}{10^{-14}M_{\odot}yr^{-1}}\right)^{0.8}\left(\frac{v_{\infty}}{400\,km\,s^{-1}}\right)^{2} \left(\frac{a}{5\,au}\right)^{-1.6}\left(\frac{\omega}{\omega_J}\right)^{0.8}\left(\frac{M_p}{M_J}\right)^{1.33}, \quad (1)$$

where $a$ is the semi-major axis of the planet's orbit in au, $\dot{M}$ ion is the stellar ionized mass-loss rate, $v_{\infty}$ is the terminal velocity of the stellar wind, and $\omega$ is the corotation speed (Farrell et al., 1999; O'Gorman et al., 2018).

Terminal velocity of stellar wind can be calculated by

$$v_{\infty} = 0.75\times617.5\times\sqrt{R_{\star}/M_{\star}},$$

where $R_{\star}$ and $M_{\star}$ are the host star radius and mass (O'Gorman et al., 2018). The radio flux density ($S_v$) emitted by an exoplanet can be estimated using the following equation

$$S_v = \frac{P_{rad}}{\Delta v \Omega d^2}, \quad (2)$$

where $P_{rad}$ is the total radio emission power of the exoplanet Equation 1, $d$ is the distance between the exoplanet and the observer, and $v$ is the maximum frequency of the radio emission,

$$v_c = 23.5\,\mathrm{MHz}\left(\frac{\omega}{\omega_J}\right)\left(\frac{M_p}{M_J}\right)^{5/3}\left(\frac{R_p}{R_J}\right)^{3},$$

where $R_p$ is the planetary radius. Substituting Equation 2 into Equation 1 gives

$$S_v = 7.6\,\mathrm{mJy}\left(\frac{\omega}{\omega_J}\right)^{-0.2}\left(\frac{M_p}{M_J}\right)^{-0.33}\left(\frac{R_p}{R_J}\right)^{-3} \left(\frac{\Omega}{1.6\,sr}\right)^{-1}\left(\frac{d}{10\,pc}\right)^{-2} \times\left(\frac{a}{1\,au}\right)^{-1.6}\left(\frac{\dot{M}_{ion}}{10^{-11}M_{\odot}yr^{-1}}\right)^{0.8}\left(\frac{v_{\infty}}{100\,km\,s^{-1}}\right)^{2}, \quad (3)$$

where $\omega_J$, $M_J$, and $R_J$, are Jupiter's corotation speed, mass, and radius and $\Omega$ is the beaming solid angle of the emission. In deriving this expression, we have followed (Farrell et al., 1999; O'Gorman et al., 2018). We assume that the planet will emit ECMI radiation within the frequency range of $\Delta v = 0.3\,v_c$ to align with the sensitivity of the SKA telescope. As a result, the coefficient in Equation 3 differs from that used in (O'Gorman et al., 2018).

The planetary corotation speed ($\omega$) is a fundamental parameter in planetary magnetospheric dynamics. In the context of close-in exoplanets, where tidal locking is prevalent due to intense gravitational forces from the host star, the corotation rate becomes particularly significant. Tidal locking occurs when the orbital period of the planet matches its rotational period, resulting in one hemisphere of the planet permanently facing the star. As a consequence, the corotation rate of tidally locked planets is synchronized with their orbital motion. This synchronization affects the generation and distribution of electromagnetic phenomena within the magnetosphere, such as auroral emissions and field-aligned currents (Zarka et al., 2001; Seager and Hui, 2002). To account for tidal locking's influence, we presume that exoplanets within orbits less than 0.1 au are tidally locked, meaning their orbital period matches their corotation period. For exoplanets beyond this threshold, we employ the Darwin-Radau relation (Murray and Dermott, 2000).

$$\omega = \sqrt{\frac{fGM_p}{R_{eq}^2}\left[\frac{5}{2}(1-1.5\,C)^2+\frac{2}{5}\right]}$$

where $C$ is 0.4 for rocky planets and 0.25 for gas giant planets and $f$ is the planet's oblateness (Hubbard, 1984). For Jovian planets with orbital distance $a < 0.1$ au, we use the oblateness of Jupiter ($f = 0.064$), and for rocky planets, we use the Earth's value which is $f = 0.00335$ (Barnes and Fortney, 2003).

## 2.2 Detectablity of the planetary radio signal

For our observations using the SKA, we focus on the SKA1-Low and SKA1-Mid frequency ranges, from 50 MHz up to 890 MHz. The imaging 1-$\sigma$ sensitivity for SKA1-Low and SKA1-Mid up to 890 MHz is detailed in Table 1, considering a continuum

TABLE 1 Image sensitivity of SKA1-Low and SKA1-mid within the indicated frequency bands for continuum observations (Braun et al., 2019).

| $\nu_{min}$ [MHz] | $\nu_{mid}$ [MHz] | $\nu_{max}$ [MHz] | $\sigma$ [$\mu$Jy] |
|---|---|---|---|
| 50 | 60 | 69 | 163 |
| 69 | 82 | 96 | 47 |
| 96 | 114 | 132 | 26 |
| 132 | 158 | 183 | 18 |
| 183 | 218 | 253 | 14 |
| 253 | 302 | 350 | 11 |
| 350 | 410 | 480 | 16.8 |
| 480 | 560 | 650 | 8.1 |
| 650 | 770 | 890 | 4.4 |

observation with a fractional bandwidth of approximately $\Delta\nu/\nu_c \approx 0.3$, alongside an integration time of 1 h.

We use the SKA image sensitivity for different ranges of frequencies as summarized in 1.

## 3 Results

We use the NASA Exoplanet Archive to calculate the radio flux of the confirmed exoplanets. The 83 exoplanets have essential data such as planetary radius and mass, orbital distance, host star radius and mass, and the system's distance from us information. To estimate $\dot{M}_{\rm ion}$, we utilized typical mass loss ratios associated with the spectral types of the host stars (Michaud et al., 2011; Puls et al., 1996; Krtička, 2014; Wood et al., 2001; Wargelin and Drake, 2002). According to our analysis, Exoplanets Qatar-4 b, TOI-1278 b, CoRoT-10 b, and HAT-P-20 b exhibit radio emissions that are detectable by the SKA telescope. All these four exoplanets are considered as close-in exoplanets:

- TOI-1278 b is a brown dwarf orbiting an M-type star. It has a mass about 18.5 times that of Jupiter and completes its orbit in approximately 14.5 days at a distance of 0.095 au (Artigau et al., 2021). Its estimated radio flux is $85.24 \pm 29.88 \times 10^2\,\mu$Jy, peaking at a frequency of $71 \pm 25$ MHz.
- CoRoT-10 b is classified as a hot/warm Jupiter, with a mass of $2.75\,M_J$. It orbits a K-type star with a period of 13.2 days (Hellier et al., 2019). Its estimated radio flux is $19.24 \pm 2.9\,\mu$Jy, with a peak frequency of $229 \pm 46$ MHz.
- Qatar-4 b is another hot Jupiter, significantly more massive at $6.1\,M_J$, and it also orbits a K-type star, completing its orbit in just 1.8 days (Alsubai et al., 2017). Its estimated radio flux is $331.31 \pm 59.7\,\mu$Jy, peaking at a frequency of $76 \pm 14$ MHz.
- HAT-P-20 b, yet another hot Jupiter, has a mass of $7.2\,M_J$ and orbits a K-type star every 2.9 days (Bakos et al., 2011). Its estimated radio flux is $20.8 \pm 1.66 \times 10^2\,\mu$Jy, with a peak frequency of $141 \pm 11$ MHz.

All these planets are massive and have short orbital distances, suggesting that mass and proximity to their stars are key factors influencing their radio emissions. Note that, for planets with orbital distances less than 0.1 au which includes these 4 planets, we assume they are tidally locked, meaning their rotation does not significantly affect their radio signals.

Figure 1 displays the distributions of planetary parameters, with exoplanets exhibiting detected radio fluxes depicted in distinct colors. In the upper-left panel, we observe that most exoplanets are situated close to their host stars, with orbital distances less than 0.1 astronomical units (au). This proximity is crucial for detecting their signals; according to the RBL model, the radio emissions from exoplanets increase as their orbital distance decreases. The upper-right panel displays the distances of these exoplanets, highlighting that all four detectable ones are located within 400 pc of Earth. For those farther away, we need to amplify their radiation to make detection possible. One promising method is to use gravitational microlensing, which can enhance the incoming radio flux, thus improving detectability (Bagheri et al., 2024b). In the lower-left panel, we present the relationship between planetary radio flux and emission frequency. The shaded area indicates the frequency range within which the SKA telescope can detect signals. The lower-right panel shows the connection between planetary flux and mass. Some exoplanets, with masses around 10 times that of Jupiter ($M_J$), exhibit very weak signals. This weakness arises from their long orbital distances, which diminish their emitted signals and make them harder to detect, as shown in the upper-left panel.

## 4 Discussion

Our understanding of planetary magnetic fields is predominantly derived from observations within our solar system. Diversifying our investigations and insights into exoplanetary magnetic fields could offer valuable perspectives on their internal dynamics and compositions. Detecting radio emissions from hot Jupiters—particularly even a single one—could provide crucial insights into how these planets respond to extreme environments and how they evolve over time. This information would greatly enhance our understanding of planetary formation, migration patterns, and the mechanisms of atmospheric escape.

In this study, employing the RBL model, we have identified four exoplanets—Qatar-4 b, TOI-1278 b, CoRoT-10 b, and HAT-P-20 b—as potential candidates for detecting radio signals using the forthcoming SKA telescope. These exoplanets are characterized as hot Jupiters. Although ECMI can be generated in hot Jupiter magnetospheres, the escape of these radio emissions from these exoplanets may be hindered by their ionospheres (Koskinen et al., 2013; Weber et al., 2017). The generation of ECMI requires a specific balance between plasma and cyclotron frequencies, with a depleted and highly magnetized plasma being essential for emission (Grießmeier et al., 2007; Zarka et al., 2018). Close-in exoplanets experience significant atmospheric expansion due to factors like

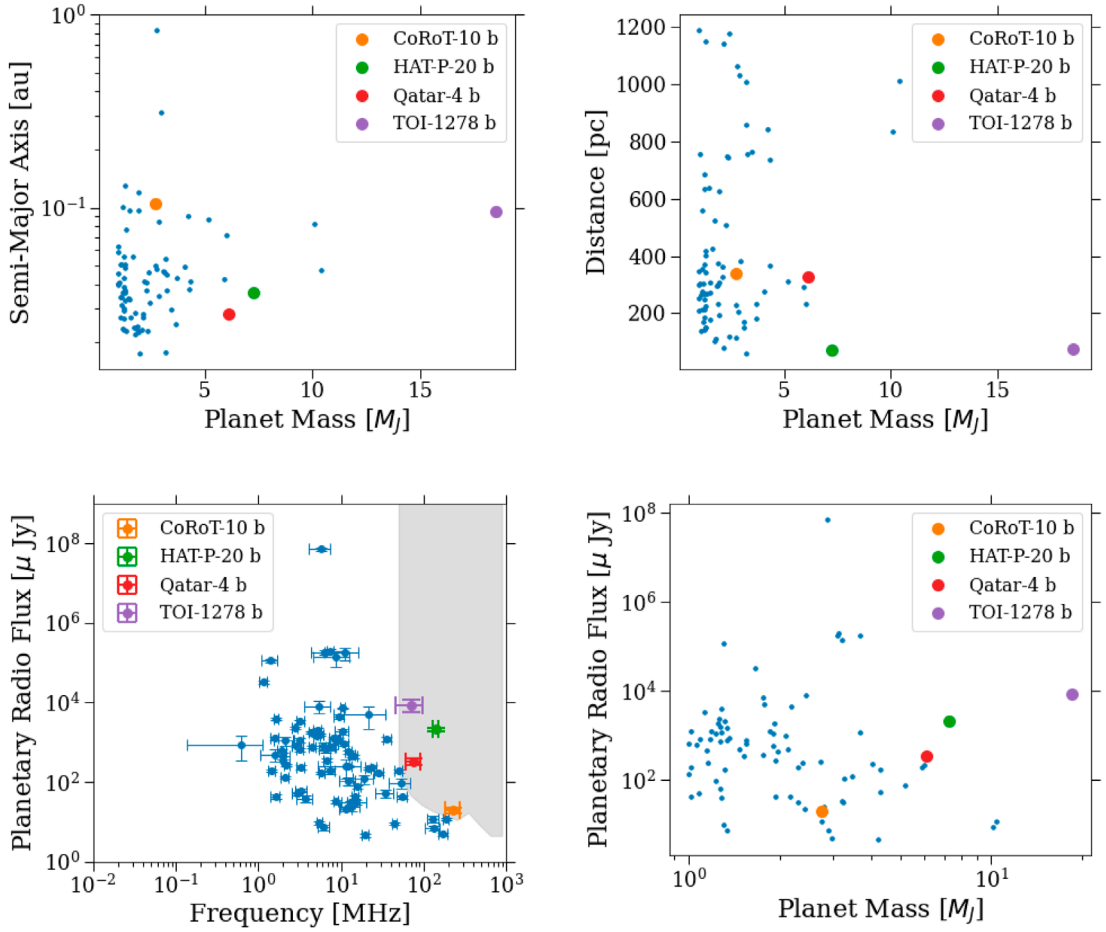


FIGURE 1
Characteristics of 83 confirmed exoplanets. Exoplanets exhibiting detectable radio signals are highlighted in different colors.

tidal forces and XUV-driven heating, leading to the formation of gaseous envelopes around the planets (Shaikhislamov et al., 2020; Johnstone et al., 2018; 2019). Studies suggest that the high plasma densities in these expanded atmospheres may prevent the escape of radio emissions or inhibit the generation of radio waves via ECMI (Weber et al., 2017). Therefore, the RBL model may not be a good estimator of the ECMI of the hot Jupiters (Bagheri et al., 2024a; Turnpenney et al., 2020). Additionally, the RBL model also does not take into account the saturation effect in the interaction between the exoplanet's magnetic field and the stellar wind's IMF. This saturation limits how much energy can be transferred from the stellar wind to the magnetosphere, as the merging rate between the two reaches a maximum threshold (Lopez, 2016; Bagheri and Lopez, 2022).

It is noticeable that a significant portion of exoplanets emitting intense radio fluxes do so at frequencies below the sensitivity range of the SKA telescope (below 50 MHz). One method to expand the detection of exoplanets with observable radio signals using current technology involves leveraging microlensing events. These events act as natural amplifiers, their magnification unaffected by the radiation's wavelength. A notable characteristic of gravitational lensing is the preservation of radiation polarization during the event. Unlike unpolarized stellar plasma radiation, radio emissions from exoplanets exhibit circular polarization (Zarka et al., 2014). Consequently, microlensing events offer a potential means to enhance the detection of exoplanets with observable radio signals (Bagheri et al., 2019; Bagheri et al., 2024b).

Understanding the magnetic fields and magnetospheric emissions of exoplanets represents a cutting-edge scientific frontier for the coming decade, as emphasized in the Origins, Worlds, and Life Planetary Science and Astrobiology Decadal Survey report. This report identifies two Priority Science Question Topics that encompass aspects of planetary magnetic fields and their interaction with the solar wind. These topics are labeled as Q6: "Solid Body Atmospheres, Exospheres, Magnetospheres, and Climate Evolution" and Q12.7: "Exoplanets, Giant Planet Structure and Eevolution" (National Academies of Sciences and Medicine, 2023).

## Data availability statement

Publicly available datasets were analyzed in this study. This data can be found here: NASA Exoplanet Archive.

## Author contributions

FB: Conceptualization, Data curation, Formal Analysis, Funding acquisition, Investigation, Methodology, Project administration, Resources, Supervision, Validation, Visualization, Writing–original draft, Writing–review and editing. AG: Data curation, Methodology, Writing–review and editing. RL: Project administration, Supervision, Writing–review and editing.

## Funding

The author(s) declare that financial support was received for the research, authorship, and/or publication of this article. We acknowledge the support of the US National Science Foundation (NSF) under Grant No. 2138122.

## Conflict of interest

The authors declare that the research was conducted in the absence of any commercial or financial relationships that could be construed as a potential conflict of interest.

## Publisher's note



## References

Alsubai, K., Mislis, D., Tsvetanov, Z. I., Latham, D. W., Bieryla, A., Buchhave, L. A., et al. (2017). Qatar exoplanet survey: Qatar-3b, Qatar-4b, and Qatar-5b. *Astronomical J.* 153, 200. doi:10.3847/1538-3881/aa6340

Artigau, É., Hébrard, G., Cadieux, C., Vandal, T., Cook, N. J., Doyon, R., et al. (2021). Toi–1278 b: spirou unveils a rare brown dwarf companion in close-in orbit around an m dwarf. *Astronomical J.* 162, 144. doi:10.3847/1538-3881/ac096d

Bagheri, F., Lopez, R., and Pham, K. (2024a). A fresh look into the interaction of exoplanets magnetosphere with stellar winds using mhd simulations. *Front. Astron. Space Sci.* 11, 1398379. doi:10.3389/fspas.2024.1398379

Bagheri, F., Lopez, R., and Shahmoradi, A. (2024b). Infrared-radio-follow-up observations for detection of the magnetic radio emission of extra solar planets: a new window to detect exoplanets. *Front. Astronomy Space Sci.* 11. doi:10.3389/fspas.2024.1400032

Bagheri, F., and Lopez, R. E. (2022). Solar wind magnetosonic mach number as a control variable for energy dissipation during magnetic storms. *Front. Astron. Space Sci.* 9, 960535. doi:10.3389/fspas.2022.960535

Bagheri, F., Sajadian, S., and Rahvar, S. (2019). Detection of exoplanet as a binary source of microlensing events in WFIRST survey. *Monthly Notices of the Royal Astronomical Society* 490 (2), 1581–1587. doi:10.1093/mnras/stz2682

Bakos, G. Á., Hartman, J., Torres, G., Latham, D. W., Kovács, G., Noyes, R. W., et al. (2011). HAT-P-20b–HAT-P-23b: four massive transiting extrasolar planets, *Astrophys. J.* 742, 116. doi:10.1088/0004-637X/742/2/116

Barnes, J. W., and Fortney, J. J. (2003). Measuring the oblateness and rotation of transiting extrasolar giant planets. *Astrophysical J.* 588, 545–556. doi:10.1086/373893

Braun, R., Bonaldi, A., Bourke, T., Keane, E., and Wagg, J. (2019). Anticipated performance of the square kilometre array–phase 1 (ska1). *arXiv Prepr. arXiv:1912.12699*. doi:10.48550/arXiv.1912.12699

Dulk, G. A. (1985). Radio emission from the sun and stars. *Annu. Rev. astronomy astrophysics* 23, 169–224. doi:10.1146/annurev.aa.23.090185.001125

Farrell, W., Desch, M., and Zarka, P. (1999). On the possibility of coherent cyclotron emission from extrasolar planets. *J. Geophys. Res. Planets* 104, 14025–14032. doi:10.1029/1998je900050

Grießmeier, J.-M., Zarka, P., and Spreeuw, H. (2007). Predicting low-frequency radio fluxes of known extrasolar planets. *Astron. Astrophys.* 475, 359–368. doi:10.1051/0004-6361:20077397

Hellier, C., Anderson, D., Bouchy, F., Burdanov, A., Cameron, A. C., Delrez, L., et al. (2019). New transiting hot jupiters discovered by wasp-south, euler/coralie, and trappist-south. *Mon. Notices R. Astronomical Soc.* 482, 1379–1391. doi:10.1093/mnras/sty2741

Hubbard, W. B. (1984). *Planetary interiors*. New York: Van Nostrand Reinhold.

Johnstone, C., Khodachenko, M., Lüftinger, T., Kislyakova, K., Lammer, H., and Güdel, M. (2019). Extreme hydrodynamic losses of earth-like atmospheres in the habitable zones of very active stars. *Astron. Astrophys.* 624, L10. doi:10.1051/0004-6361/201935279

Johnstone, C. P., Güdel, M., Lammer, H., and Kislyakova, K. G. (2018). Upper atmospheres of terrestrial planets: carbon dioxide cooling and the earth's thermospheric evolution. *Astron. Astrophys.* 617, A107. doi:10.1051/0004-6361/201832776

Koskinen, T., Harris, M., Yelle, R., and Lavvas, P. (2013). The escape of heavy atoms from the ionosphere of hd209458b. i. a photochemical–dynamical model of the thermosphere. *Icarus* 226, 1678–1694. doi:10.1016/j.icarus.2012.09.027

Krtička, J. (2014). Mass loss in main-sequence b stars. *Astron. Astrophys.* 564, A70. doi:10.1051/0004-6361/201321980

Lazio, J., Hall, P., Schilizzi, R., and Lazio, T. (2009). The square kilometre array. *Proc. IEEE* 97, 1482–1496. Dataset. doi:10.1109/jproc.2009.2021005

Lazio, J., Hallinan, G., Airapetian, V., Brain, D., Dong, C., Driscoll, P., et al. (2018). Magnetic fields of extrasolar planets: planetary interiors and habitability. *arXiv Prepr. arXiv:1803.06487*. doi:10.48550/arXiv.1803.06487

Lopez, R. E. (2016). The integrated dayside merging rate is controlled primarily by the solar wind. *Journal of Geophysical Research: Space Physics* 121, 4435–4445.

Melrose, D., and Dulk, G. A. (1982). Electron-cyclotron masers as the source of certain solar and stellar radio bursts. *Astrophysical J.* 259, 844–858. doi:10.1086/160219

Michaud, G., Richer, J., and Vick, M. (2011). Sirius a: turbulence or mass loss? *Astron. Astrophys.* 534, A18. doi:10.1051/0004-6361/201116999

Murphy, T., Bell, M. E., Kaplan, D. L., Gaensler, B., Offringa, A. R., Lenc, E., et al. (2015). Limits on low-frequency radio emission from southern exoplanets with the murchison widefield array. *Mon. Notices R. Astronomical Soc.* 446, 2560–2565. doi:10.1093/mnras/stu2253

Murray, C. D., and Dermott, S. F. (2000). *Solar system dynamics*. Cambridge University Press.

National Academies of Sciences, E. and Medicine (2023). *Origins, Worlds, and life: planetary science and Astrobiology in the next decade*. Washington, DC: The National Academies Press. doi:10.17226/27209

Noyola, J., Satyal, S., and Musielak, Z. (2016). On the radio detection of multiple-exomoon systems due to plasma torus sharing. *Astrophysical J.* 821, 97. doi:10.3847/0004-637x/821/2/97

Noyola, J. P., Satyal, S., and Musielak, Z. E. (2014). Detection of exomoons through observation of radio emissions. *Astrophysical J.* 791, 25. doi:10.1088/0004-637x/791/1/25

O'Gorman, E., Coughlan, C. P., Vlemmings, W., Varenius, E., Sirothia, S., Ray, T. P., et al. (2018). A search for radio emission from exoplanets around evolved stars. *Astron. Astrophys.* 612, A52. doi:10.1051/0004-6361/201731965

Puls, J., Kudritzki, R.-P., Herrero, A., Pauldrach, A., Haser, S., Lennon, D., et al. (1996). O-star mass-loss and wind momentum rates in the galaxy and the magellanic clouds observations and theoretical predictions. *Astronomy Astrophysics* 305, 171. doi:10.1051/0004-6361/201731965

Seager, S., and Hui, L. (2002). Constraining the rotation rate of transiting extrasolar planets by oblateness measurements. *Astrophysical J.* 574, 1004–1010. doi:10.1086/340994

Shaikhislamov, I., Khodachenko, M., Lammer, H., Berezutsky, A., Miroshnichenko, I., and Rumenskikh, M. (2020). Three-dimensional modelling of absorption by various species for hot jupiter hd 209458b. *Mon. Notices R. Astronomical Soc.* 491, 3435–3447. doi:10.1093/mnras/stz3211

Turner, J. D., Zarka, P., Grießmeier, J.-M., Lazio, J., Cecconi, B., Enriquez, J. E., et al. (2021). The search for radio emission from the exoplanetary systems 55 cancri,

υ andromedae, and τ boötis using lofar beam-formed observations. *Astron. Astrophys.* 645, A59. doi:10.1051/0004-6361/201937201

Turnpenney, S., Nichols, J. D., Wynn, G. A., and Jia, X. (2020). Magnetohydrodynamic modelling of star–planet interaction and associated auroral radio emission. *Mon. Notices R. Astronomical Soc.* 494, 5044–5055. doi:10.1093/mnras/staa824

Wargelin, B. J., and Drake, J. J. (2002). Stringent x-ray constraints on mass loss from proxima centauri. *Astrophysical J.* 578, 503–514. doi:10.1086/342270

Weber, C., Lammer, H., Shaikhislamov, I. F., Chadney, J., Khodachenko, M., Grießmeier, J.-M., et al. (2017). How expanded ionospheres of hot jupiters can prevent escape of radio emission generated by the cyclotron maser instability. *Mon. Notices R. Astronomical Soc.* 469, 3505–3517. doi:10.1093/mnras/stx1099

Wood, B. E., Linsky, J. L., Müller, H.-R., and Zank, G. P. (2001). Observational estimates for the mass-loss rates of Observational Estimates for the Mass-Loss Rates of α Centauri and Proxima Centauri Using [ITAL]Hubble Space Telescope[/ITAL] L[CLC]y[/CLC]α Spectra centauri and proxima centauri using hubble space telescope lyα spectra. *Astrophysical J.* 547, L49–L52. doi:10.1086/318888

Zarka, P. (1998). Auroral radio emissions at the outer planets: observations and theories. *J. Geophys. Res. Planets* 103, 20159–20194. doi:10.1029/98je01323

Zarka, P. (2004). Fast radio imaging of jupiter's magnetosphere at low-frequencies with lofar. *Planet. Space Sci.* 52, 1455–1467. doi:10.1016/j.pss.2004.09.017

Zarka, P. (2007). Plasma interactions of exoplanets with their parent star and associated radio emissions. *Planet. Space Sci.* 55, 598–617. doi:10.1016/j.pss.2006.05.045

Zarka, P., Lazio, T. J. W., and Hallinan, G. (2014). Magnetospheric radio emissions from exoplanets with the ska

Zarka, P., Marques, M., Louis, C., Ryabov, V., Lamy, L., Echer, E., et al. (2018). Jupiter radio emission induced by ganymede and consequences for the radio detection of exoplanets. *Astron. Astrophys.* 618, A84. doi:10.1051/0004-6361/201833586

Zarka, P., Treumann, R. A., Ryabov, B. P., and Ryabov, V. B. (2001). "Magnetically-driven planetary radio emissions and application to extrasolar planets," in *Physics of space: growth points and problems* (Springer), 293–300.